2008

Force interaction characterization between thrombin and DNA aptamers

Janice Dionne Marquardt
Iowa State University

Force interaction characterization between thrombin and DNA aptamers

By

Janice Dionne Marquardt

A thesis submitted to the graduate faculty
in partial fulfillment of the requirements for the degree of
MASTER OF SCIENCE

Major: Mechanical Engineering

Program of Study Committee:
Pranav Shrotriya, Major Professor
Sriram Sundararajan
Marit Nilsen-Hamilton

Iowa State University
Ames, Iowa
2008

Table of Contents

List of Figures

List of Tables

Chapter 1: Introduction

With so much research in progress to study biomedical applications of engineering principles, sensor systems are quickly becoming a primary bridge between biology and engineering. One of the most common applications for these sensors is to detect concentrations of chemical species, with the goal of detecting ever-smaller concentrations with ever-greater certainty and specificity. This thesis specifically studies the detection and binding forces of the protein thrombin using a single-stranded DNA aptamer as the detection mechanism. The two methods employed to measure the interaction between the thrombin and its corresponding DNA aptamer were microcontact printing and force spectroscopy. Based on these experiments, a characterization of thrombin and the aptamer was completed.

This thesis is organized into four chapters. This first chapter provides a background of the biochemical and mechanical principles discussed in chapters two and three. Chapter two is a research letter resulting from microcontact printing research, and will be submitted to *Nano Letters*. Chapter three is a research paper resulting from force spectroscopy research, and is to be submitted to *Langmuir*. Chapter four discusses general conclusions drawn from this research and proposes future work in regards to these topics.

Relevant Biochemistry Background

Deoxyribose Nucleic Acid (DNA)

In the early 1950s, James Watson and Francis Crick proposed a structure for the fundamental chemical species that governs daily life for all creatures: Deoxyribose Nucleic Acid (DNA) (Watson & Crick, 1953). This helical double strand made up of four nucleic acids—adenine, thymine, guanine, and cytosine—forms the backbone of modern biochemistry. DNA has an approximate "footprint" of 2.4 nm by 2.2 nm, and a length of 0.34 nm per base pair. Each base pair is also asymmetrical and so a strand of DNA has a five prime (5') end, which terminates in a phosphate group; and a three prime (3') end, which terminates in a hydroxyl group. As a double-stranded helix, DNA is quite rigid and forms rod-like shapes. DNA can also be manufactured as a single strand, without a typical inherent structure of its own. Single-stranded DNA (ssDNA) can form many different shapes and

structures based on its base sequence, and usually different structure than double stranded DNA.

Aptamers

One of the more recent applications of single-stranded DNA is to form structures known as aptamers (Cullen & Greene, 1989; Ellington & Szostak, 1990). Aptamers are engineered nucleic acid strands that are selected using the Systematic Evolution of Ligands by Exponential Enrichment (SELEX) method due to their ability to bind a specific protein (Tuerk & Gold, 1990). These aptamers can then be used to detect the protein's presence through assays, to be immobilized in arrays, or to inhibit the protein's inherent function. Aptamers are flexible and versatile molecules with a wide range of biochemical applications.

The specific aptamer used in this study was developed by Tasset, et al. to bind to the protein human thrombin (Tasset, Kubik, & Steiner, 1997). The thrombin aptamer has a hairpin structure formed by eight guanine bases, which form what is known as a G-quadruplex (Macaya, Schultze, Smith, Roe, & Feigon, 1993). The G-quadruplex has the base structure $GGNTGGN_2$-$_5$GGNTGG, which fits into thrombin's heparin binding site (Kelly, Feigon, & Yeates, 1996). In Figure 1, the guanine bases are represented by the white spheres and the hydrogen bonds that hold the hairpin together are the gray rods. The black backbone is the rest of the ssDNA strand, which can be of various lengths depending on the intended application of the aptamer. The 3' and 5' labels represent the 3' end and 5' end of the DNA strand, respectively, although the aptamer extension can be on either the 3' or 5' end without significantly changing the aptamer function.

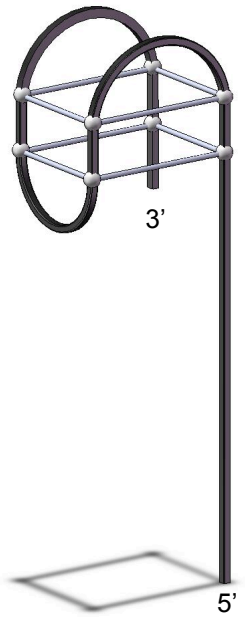

Figure 1: Thrombin Aptamer Structure

It is hypothesized that the thrombin aptamer binds to thrombin with a physical rather than chemical bonding process, where the structure of the thrombin creates a place for the hairpin to "hook" into the protein (Basnar, Elnathan, & Willner, 2006; Tasset, Kubik, & Steiner, 1997). The dissociation constant—the propensity of the thrombin-aptamer complex

to separate—of the thrombin aptamer is around 75 nM, with some experiments finding it as low as 1.4 nM (Macaya, Schultze, Smith, Roe, & Feigon, 1993; Tsiang, Gibbs, Griffin, Dunn, & Leung, 1995). This shows that the thrombin aptamer has high specific bonding to thrombin.

When the aptamer binds with thrombin, either end of the aptamer can be modified by labeling with fluorescent or dye groups, or to immobilize the aptamer-protein complex. In this study, a thiol group consisting of a sulfur-hydrogen pair was added to the 5' end of the aptamer in order to immobilize it on a gold surface. The thiol group has a high affinity for gold, and forms a strong bond with a gold substrate with a Gibbs free energy on the order of 23 kJ/mol (Yang, Yau, & Chan, 1998). With this thrombin aptamer structure, the protein can be immobilized on a flat gold surface for further scanning and experimentation to analyze its behavior and properties.

Thrombin

Human thrombin is a blood coagulation protein that acts as a catalyst in many reactions, including the conversion of fibrinogen into fibrin. Fibrinogen, synthesized in the liver, can be converted into fibrin to form a mesh that is part of the blood clotting process. Thrombosis is one disease that results from too much fibrin in the system, which can also be caused by too much thrombin. The opposite, hemorrhage, results from not enough fibrin and can be caused by too little thrombin as well as other factors. Therefore, the study and control of thrombin is vital to the blood coagulation process and human health.

Human thrombin has two major binding sites that are relevant to this study (Bode et al., 1989). The first site is the fibrinogen binding site, which is where the cleavaged fibrinogen to fibrin occurs. This site is primary to thrombin's function in the bloodstream. The second site is the heparin binding site, which is where the molecule heparin binds to the thrombin and inhibits its function. Heparin is found in the saliva of leeches, and its interaction with thrombin explains the anti-coagulation properties of leeches. When heparin is present, the ability of thrombin to cleave fibrinogen is drastically reduced. In the presence of the thrombin aptamer, fibrin production has been shown to slow by as much as 675% (Bock, Griffin, Latham, Vermaas, & Toole, 1992).

This slowing of fibrin production indicates that the aptamer affects the thrombin in a similar way to heparin. It is hypothesized the heparin binding site primarily binds to the thrombin aptamer. However, the presence of the thrombin aptamer in the fibrinogen binding site could also slow fibrin production.

Motivation

In detecting biological species, small samples and high sensitivity are key. In the human system, small changes can elicit large responses and result in potentially fatal illnesses. Many custom chemical species are expensive and difficult to manufacture, so a small sample size can save in research costs and can also reduce final sensor costs.

This thesis serves as a proof-of-concept for small-scale sensor systems that do not use fluorescence to detect bonding. Fluorescence is a common type of labeling, which is where chemical species are modified with an additional molecule that emits a visual signal at a binding event. Most commonly, labels will be attached at the binding site of a species, where they are released upon binding. The released label will give off a detectable signal, frequently visual. Chemical species that have been labeled are more expensive to manufacture, and are limited in their sensor applicability. Nonlabeled species require less handling, and a method of detection for nonlabeled aptamers would prove more versatile for sensing applications.

Most current sensors utilize fluorescence to detect the presence or absence of chemical species. In the fluorescence method, the DNA aptamers are functionalized with fluorescent groups that put out a visual signal that changes luminescence when binding with their complimentary chemical species. This detection can be used with fixed or free aptamers, but can only be used for surfaces without an inherent fluorescence (C. L. Feng, Embrechts, Vancso, & Schönherr, 2006; X.-z. Feng et al., 2004; Lee et al., 2007).

The most common fabrication method for sensor arrays with biological and chemical species still relies on printed patterns where binding is detected using fluorescence (Kumar & Whitesides, 1993; Mrksich & Whitesides, 1995; Ruiz & Chen, 2007; Xia & Whitesides, 1998). The issue with these sensors is that they require a non-luminescent substrate such as glass or mica. A sensor system that does not use fluorescence would have the flexibility to

use substrates such as gold, protein, or polymers in addition to glass or mica for immobilization.

Other printed or otherwise immobilized species arrays include a surface acoustic wave (SAW) sensor (Gronewold, Glass, Quandt, & Famulok, 2005), charge transfer sensor (Hianik, 2005), or microcantilever sensor (Lavrik, Sepaniak, & Datskos, 2004). The SAW sensors measure changes in acoustic waves that are translated through the substrate. The amplitude and velocity change between binding events, which indicates the presence of the bound chemical species. The charge transfer sensors measure changes in electrochemical response using an indicator such as methylene blue (Hianik, 2005), but this sensor still requires dye sensing much like fluorescence methods. Microcantilever sensors use small cantilevers (approx. 2 nm thick by 400 nm long) to measure surface stress changes across the cantilever surface. As the surface stress changes due to protein binding, the cantilever produces a physical response that can be measured using laser interferometry or vibration harmonics (Lavrik, Sepaniak, & Datskos, 2004). Sensors using free aptamers are in the form of chemical assays, and still rely on dyes or luminescence for detection (Olsen & Markwell, 2007)

Microcontact Printing Background

One of the most widespread methods for creating micro and nanoscale structures was first outlined by Kumar and Whitesides, who described an "inking" process of transferring alkanethiols to gold surfaces (Kumar & Whitesides, 1993). Known as microcontact printing, this process has been used to print a multitude of chemical species from cell cultures to proteins to DNA (X.-z. Feng et al., 2004; Mrksich & Whitesides, 1995; Xia & Whitesides, 1998).

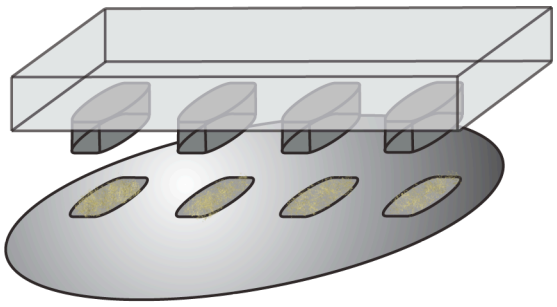

Figure 2: Microcontact printing process. Not to scale.

To perform microcontact printing, a flexible polymer poly(dimethyl siloxane) (PDMS) stamp is made from a mold. The chemical species is exposed to the stamp as a solution in liquid, and then the liquid is either allowed to

dry (as in the case of alcohol based solutions) or is dried with a gas such as nitrogen (as in the case of water based solutions). The dried chemical species is then printed on a substrate, where it adheres or bonds to the substrate. The PDMS stamp is removed, leaving a pattern of the chemical species printed on the substrate (see Figure 2).

This bottom-up fabrication mechanism is frequently used for masking substrates to create patterns and molds, but it can also be used to form the base for self-assembled biological or chemical structures. The printed chemical species forms the initial layer for the intended structure, and future layers "self-assemble" based on their binding specificity to the preceding layer.

In using microcontact printing for sensing systems, a known pattern (such as a grid of squares) of a chemical species is printed onto a substrate. A solution containing a complementary species is exposed to the substrate, and the complementary species bonds only to the printed species. In the case of fluorescence, the printed species has a fluorescent "tag" on the binding end, which is reoriented upon binding to the species in the solution. It is this fluorescence that can be detected with luminescence detectors and forms a visible pattern on the substrate. In this thesis, the presence of the complementary species is detected by measuring the height change before and after exposure to the solution containing the complementary species.

Force Spectroscopy Background

In determining the applicability of certain complimentary chemical species to sensor systems, it is vital to know the specificity of the binding between the species. One of the measures of this specificity is based on the force interaction between the complimentary pair. While the atomic force microscope (AFM) is most commonly used to measure topography data of small scans, it can also be used for other applications such as force measurements. For normal scanning functions, the AFM utilizes a detector and triangular

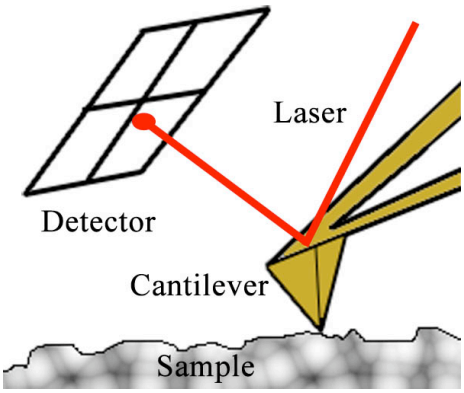

Figure 3: AFM function schematic

cantilever system to measure micro- and nanoscale data (see Figure 3). A laser beam is deflected off of the cantilever onto a photodetector, which registers changes in the cantilever's position. At the same time, the cantilever moves across the sample, reacting to topographical changes as it scans. The data is compiled line by line until a complete topographical map has been created.

In the case of force spectroscopy, the cantilever does not move across the sample, and instead moves vertically in one place. This method measures the cantilever's deflection based in its interaction with the surface to create what is known as a force curve. The deflections measured in a force curve can be converted into forces by using the cantilever's spring constant.

The method known as force spectroscopy—or force microscopy—was first introduced in 1994 (Florin, Moy, & Gaub, 1994). Florin et al. investigated the forces of the complimentary species avidin and biotin through the use of force spectroscopy. In this method, the first chemical species is bound to an AFM cantilever tip through carboxyl chemistry, thiol groups (Basnar, Elnathan, & Willner, 2006), biotinylated groups (Florin, Moy, & Gaub, 1994; Micic, Chen, Leblanc, & Moy, 1999), or other methods. The complementary species is then bound to a flat substrate using similar methods (See Figure 4). The binding of each species to its substrate must have a much stronger binding force than that of the complementary species, in order to avoid measuring the binding forces of the chemical species to the substrates.

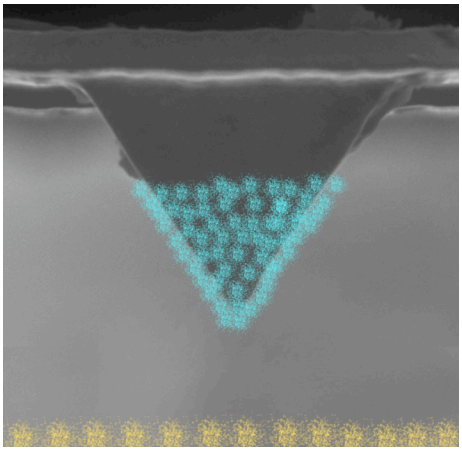

Figure 4: Functionalized tip and substrate. Not to scale.

After preparation of all surfaces, the cantilever and substrate are brought together and then pulled apart using force curves. This causes the complementary species to bind, stretch, and finally separate. The deflection of the cantilever indicates the point of contact with the substrate, the stretching, and the breaking forces. The force spectroscopy method is used to directly measure the binding forces between complementary species, and is especially applicable to manufactured complementary pairs such as aptamers.

From an engineering standpoint, the forces between thrombin and its binding agents are vital to the design of sensor systems. In particular, the magnitudes of the forces dictate the suitability of certain sensors to the detection of thrombin. While the microcontact printing sensor system described in this thesis relies on height rather than forces to measure the presence of thrombin, other sensor systems rely on surface stress changes or interaction forces to trigger a detection sequence (Lavrik, Sepaniak, & Datskos, 2004).

Contact Mechanics

When calculating forces in a force spectroscopy experiment, attention to the area in contact during the binding phase is vital. The most common method of calculating the contact area between a spherical and flat surface was developed by Hertz in the late 1800s as described in (Johnson, 1985). This method does not include small-scale adhesion forces, but does include elastic deformation due to the normal force with which the two surfaces are brought into contact. Most researchers choose to use the Hertz contact analysis as an initial contact area estimation, and some do not analyze the system much further as they argue that deformation does not play a strong role in force spectroscopy interactions (Noy, Vezenov, & Lieber, 1997).

Some researchers then do go on to calculate the contact area based on other methods, which take adhesion forces into account (Chandross, Lorenz, Stevens, & Grest, 2008; Goss, Brumfield, Irene, & Murray, 1993; Kopycinska-Müller, Geiss, & Hurley, 2005; Noy, Vezenov, & Lieber, 1997; Oncins, Vericat, & Sanz, 2008). The general consensus is that while the DMT method (Derjaguin-Muller-Toporov) more accurately models the work of adhesion, the JKR method (Johnson-Kendall-Roberts) is better for the surface profile and contact area calculations when adhesion forces will be taken into consideration.

Most researchers conclude that neither of these models truly captures the contact mechanics on this scale well and a few have proposed their own models for interactions with thin films (Dimitriadis, Horkay, Maresca, Kachar, & Chadwick, 2002; Reedy, 2006). These contact models do not involve protein or DNA monolayers, and are highly specific. In force spectroscopy, the specific species of the experiment determine the most appropriate contact model. This is because the thicknesses of the layers on the AFM tip and substrate and the

medium of the experiment (such as liquid, air, or vacuum) have a large impact on the magnitude of the secondary forces such as meniscus and Van der Waals forces.

Current Work

The current work described in this thesis combines the principles of thrombin and nucleic acid biochemistry, biosensors, atomic force microscopy, and contact mechanics. The first experiment conducted to characterize the thrombin-aptamer interactions was to create a biosensor using microcontact printing. Using the atomic force microscope to measure height changes, it was shown that a printed array can serve as a biosensor without the use of fluorescence. More details on this experiment can be found in chapter two.

The second experiment conducted was to determine the force of the aptamer-thrombin interaction through the use of force spectroscopy. Here the atomic force microscope was used to measure cantilever deflection rather than height changes as we repeated the work of Basnar et al. (Basnar, Elnathan, & Willner, 2006). More details on this experiment can be found in chapter three.

Based on the two experiments conducted, we reached some general conclusions about the thrombin-aptamer interaction characteristics. These conclusions as well as suggestions for future research can be found in chapter four. During the course of the force spectroscopy experiment, an interesting poly(ethylene) glycol superstructure was observed on the substrate surface. Details of this observation can be found in Appendix A.

For each of the papers in this thesis, Janice Marquardt was the primary author and researcher. Dr. Pranav Shrotriya provided guidance, some data analysis programming, and editing; and he is the author for correspondence. Dr. Marit Nilsen-Hamilton provided biochemistry expertise and editing. Kanaga Karuppiah fabricated the stamp used in the microcontact printing experiment.

Chapter 2: Microcontact printing to detect thrombin binding to DNA aptamers with applications to biosensor systems

Modified from a paper to be submitted to *Nano Letters*

Janice Marquardt, Pranav Shrotriya, Marit Nilsen-Hamilton

Abstract

As the use of chemical species to form nanostructures becomes ever more common, the need to detect binding specificity of these species also increases. Many sensor systems require modification of the binding molecules to add fluorophones to one or both molecules, which is costly and requires a non-fluorescent substrate for the binding activity. The purpose of this study is to examine the feasibility of using atomic force microscope (AFM) height measurements to detect changes in nucleic acid and protein interactions. This study used a thiolated 30-nt adenine oligonucleotide (Poly A) and its corresponding thymine DNA strand (Poly T) as a control, and the thiolated thrombin DNA aptamer and thrombin for the targeted detection pair. The poly A and aptamer were printed using microcontact printing techniques onto gold, and then were exposed to their complementary species. It was shown that there was a height change after binding to the target species, so it is feasible to use height data to detect binding of DNA aptamers and proteins. This fluorescence-free sensor system uses unmodified proteins, and so has far-reaching applications for sensing protein binding and building nanostructures.

Introduction

Biosensors have far-reaching applications in the fields of security, medicine, and many other fields where detections of small quantities of substances are necessary. Research using biological building blocks to create these sensors is exploring the possibilities of small scale sensing to detect abnormalities and create complex structures.

A small-scale sensor has many advantages, including its fine sensitivity. A micro or nanoscale sensor can detect very small concentrations of chemical species, and has high specificity. As the sensor decreases in size, the necessary sample size likewise decreases. The sensor in this paper uses a less than 100 uL sample size.

To reliably detect biological and chemical species on small scales, a highly specific sensor is needed to minimize error. One of the more recent advances in DNA technology is the creation of single-stranded DNA aptamers, which are selected from a random pool of nucleotide chains and often further engineered to bind to a specific protein (Cullen & Greene, 1989). These aptamers can be used with sensor systems to detect certain proteins and bind them to certain surfaces, or they can be used to inhibit the activities of the proteins (Tasset, Kubik, & Steiner, 1997). Aptamers are at the lower end of the nanoscale, with a diameter of 2-3 nm and length of 5-20 nm, which gives them great flexibility for a variety of applications.

One of the most common methods for creating micro and nanoscale structures was first outlined by Kumar and Whitesides, who described an "inking" process of transferring alkanethiols to gold surfaces (Kumar & Whitesides, 1993). Known as microcontact printing, this process has been used to print a multitude of chemical species from cell cultures to proteins to DNA (X.-z. Feng et al., 2004; Mrksich & Whitesides, 1995; Xia & Whitesides, 1998). This bottom-up fabrication mechanism is frequently used for masking substrates to create patterns and molds, but it can also be used to form the base for a self-assembled biological or chemical structure. The printed chemical species forms the initial layer for the intended structure, and future layers "self-assemble" based on their binding specificity to the preceding layer.

Self-assembled monolayers of DNA strands are especially useful for creating complicated nanostructures several layers high in microcontact printing (Zhou, Bruckbauer, Ying, Abel, & Klenerman, 2003). A self-assembled monolayer is made up of DNA strands packed very closely to form a dense group of standing DNA molecules. Zhou et al. observed imperfect monolayers and DNA that did not exhibit the ideal upright structure that results in close-packed strands (Zhou, Bruckbauer, Ying, Abel, & Klenerman, 2003). Therefore, the measured height of their nanostructures more closely corresponded to the diameter of the DNA than to the length of the strands.

The current intersection of microcontact printing and biosensors frequently utilizes fluorescence to detect the presence or absence of chemical species. In this method, the DNA aptamers are functionalized with fluorescent groups that put out a visual signal when they

bind with their complimentary chemical species. This detection can be used with fixed or free aptamers, but can only be used for surfaces without an inherent fluorescence such as glass or mica (C. L. Feng, Embrechts, Vancso, & Schönherr, 2006; X.-z. Feng et al., 2004; Lee et al., 2007).

While glass is a useful medium for fluorescence detection, gold cannot be used in fluorescence because of its inherent luminescence. Last, the "glow" from fluorescence can result in errors in measurement based on the size of the measured species. The halo around the measured species can change its measured size, or its measured density in the case of closely-packed molecules.

In this letter, we report a proof of concept on a sensor system using the atomic force microscope (AFM) to identify specific aptamers and verify their binding ability. The reported method uses printing of thiolated aptamers (a sulfur-hydrogen sequence with a strong affinity for gold) on a gold substrate, followed by detection of the height change caused by binding to the target protein. Complementary DNA strands were also printed to serve as a control for validation of the printing process and to expand its validity to other binding combinations.

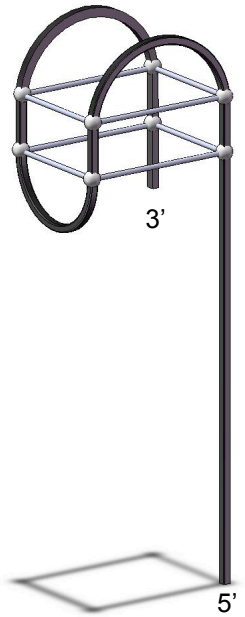

Figure 5: Thrombin Aptamer Structure

This study uses an aptamer selected by Tasset, et al., which binds to the blood coagulation thrombin (Tasset, Kubik et al. 1997). The thrombin aptamer includes 15 nucleotides that form a "hairpin" pattern (see Figure 5) that binds to the heparin binding site on a thrombin protein (Tasset, Kubik, & Steiner, 1997). In Figure 1, the white spheres represent the guanine molecules that form the cornerstones of the G-quadruplex first documented by Bock, et al (Bock, Griffin, Latham, Vermaas, & Toole, 1992). The light gray bonds represent the hydrogen bonding to form the actual quadruplex structure that creates a physical bond to the thrombin molecule (Macaya, Schultze, Smith, Roe, & Feigon, 1993). Here the minimal 15-nt sequence for high affinity binding to thrombin was added to a 35-nt sequence of random nucleic acids

with low probability of secondary structures (Basnar, Elnathan, & Willner, 2006). This added "tail" allows the fixed thrombin aptamer enough space to bind to the thrombin molecule without an added risk of interfering secondary structures. The 5' and 3' labels in figure 5 mark the 5' and 3' ends of the single stranded DNA, respectively. Like most single strands of DNA, this aptamer should form a self-assembled monolayer under the appropriate conditions.

Methods

Unless otherwise noted, all chemicals were purchased from Sigma Aldrich (www.sigma.com), and all DNA was purchased from Integrated DNA Technologies (www.idtdna.com). Using an SU-8 photoresist master, a poly(dimethylsiloxane) mold (PDMS) was prepared with 5 μm by 5 μm squares with a 10 μm spacing. The PDMS was cured at 60°C for a minimum of 12 hours. As shown by Thibault, et al., a longer cure time (greater than 12 hours and up to 28 hours) results in a cleaner PDMS substrate (Thibault, Séverac, Mingotaud, Vieu, & Mauzac, 2007). Thibault, et al. also showed that uncleanliness of PDMS is beneficial to DNA printing due to its sponge-like composition.

To print the thiolated poly A single stranded DNA (5'-AAA AAA AAA AAA AAA AAA AAA AAA AAA AAA-thiol-3'), an 88.5 μM concentration of poly A in double distilled water (ddH_2O) was deposited on the PDMS stamp. After settling for 30 seconds, the excess liquid was poured off and the remaining liquid evaporated with a gentle stream of nitrogen. The stamp was placed on a silicon wafer with a 25 nm thick layer of sputter-coated gold for 30 seconds and then was removed. The sample was rinsed with ddH_2O and dried again before being scanned by the AFM.

To hybridize the DNA, a 50.6 μM solution of poly T DNA (5'-TTT TTT TTT TTT TTT TTT TTT TTT TTT TTT-3') in binding buffer (20 mM Tris-HCl pH 7.4, 140 nM NaCl, 5 mM KCl, 1 mM $CaCl_2$, 1 mM Mg Cl_2, and 5% glycerol v/v in ddH_2O) was added to the dry sample and allowed to remain for 30 seconds. The excess was poured off and dried with a gentle nitrogen stream. The sample was rinsed with ddH_2O before being scanned.

To print the thiolated thrombin aptamer (5'-thiol-GCC TTA ACT GTA GTA CTG GTG AAA TTG CTG CCA TT**G GTT GGT GTG GTT GG**-3'), (Tasset, Kubik, & Steiner,

1997), a solution of 3.4 μM aptamer in ddH_2O was deposited on the PDMS stamp. After settling for one minute, the excess liquid was poured off and replaced with a binding buffer (20 mM Tris-HCl pH 7.4, 140 nM NaCl, 5 mM KCl, 1 mM $CaCl_2$, 5 mM $MgCl_2$, and 5% glycerol v/v in ddH_2O). The sample was heated to 80°C for 30 minutes, then rinsed several times with the same binding buffer followed by ddH_2O. The sample was dried with a gentle stream of nitrogen before being scanned.

To bind the aptamer with thrombin, a 10 μM concentration of thrombin in high $MgCl_2$ binding buffer with Tween20 included to decrease non-specific binding (20 mM Tris-HCl pH 7.4, 140 nM NaCl, 5 mM KCl, 1 mM $CaCl_2$, 5 mM Mg Cl_2, 5% glycerol v/v and 0.05% Tween20 v/v in ddH_2O) was deposited on the printed surface. The mixture was allowed to stand for 1 minute before being rinsed several times in binding buffer with NP40 included (20 mM Tris-HCl pH 7.4, 140 nM NaCl, 5 mM KCl, 1 mM $CaCl_2$, 5 mM Mg Cl_2, 5% glycerol v/v and 0.05% NP40 v/v in ddH_2O) followed by rinsing several times with ddH_2O.

To create a control binding pair, poly A was printed and exposed to the thrombin protein. The poly A was printed using the same method as in the poly A/poly T experiment, and the thrombin was exposed to the poly A using the same method as in the aptamer/thrombin experiment. A summary of the four species used can be found in Table 1.

Table 1: Summary of chemical species used for printing

Chemical Species	Concentration	Solution
Thiolated poly A	88.5 μM	ddH_2O
Poly T	50.6 μM	20 mM Tris-HCl pH 7.4 140 nM NaCl 5 mM KCl 1 mM $CaCl_2$ 1 mM Mg Cl_2 5% glycerol v/v in ddH_2O
Thiolated Thrombin Aptamer	3.4 μM	ddH_2O
Thrombin	10 μM	20 mM Tris-HCl pH 7.4 140 nM NaCl 5 mM KCl 1 mM $CaCl_2$ 5 mM Mg Cl_2 5% glycerol v/v 0.05% Tween20 v/v in ddH_2O

Scanning of height and friction traces was conducted in air and water using silicon nitride atomic force microscope tips on a Dimension 3100 atomic force microscope. The heights of the features were calculated using the cross section function of NanoScope offline software version 5.30. The range of true heights was calculated based on fifty height measurements and a 95% confidence interval for a normally distributed data set. The heights were also calculated using average heights, with results similar to the individual measurements. Individual measurements were used because a significant number of data points could be generated for greater potential for analyses.

Results

The AFM scans shown use red as the lowest heights, and yellow to indicate peaks in height. Figures 2 and 3 show the AFM data for the four situations measured. Each image is 20 μm square with the height data on a 10 nm scale.

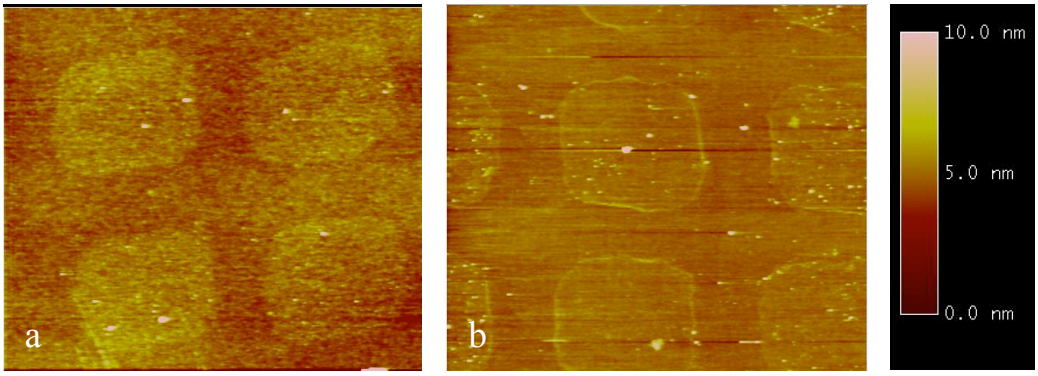

Figure 6: Poly A and T DNA AFM Height Data. a) Poly A b) Hybridized poly A and poly T

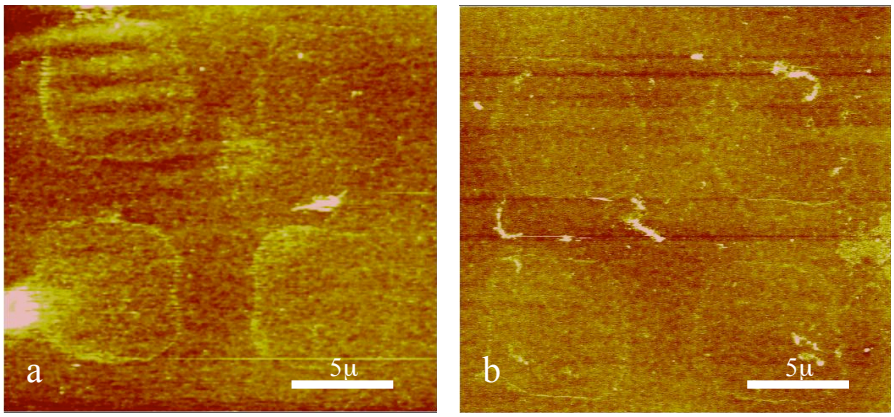

Figure 7: Thrombin aptamer AFM Height Data. a) Aptamer b) Bound thrombin

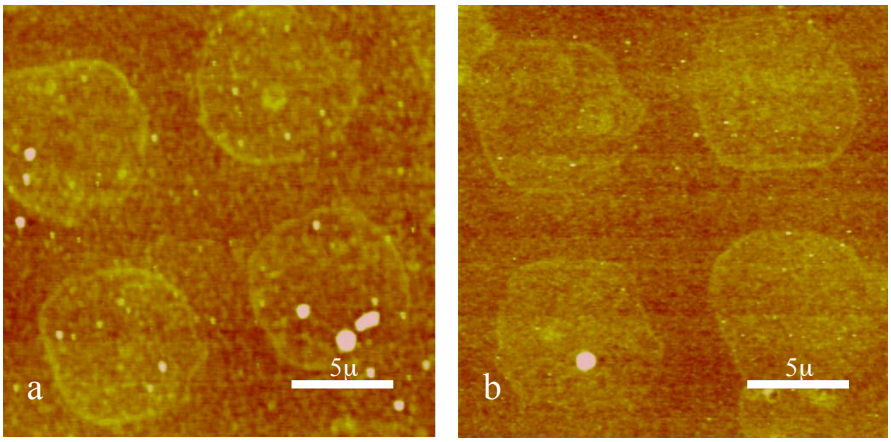

Figure 8: Control AFM Height Data. a) Poly A b) Poly A exposed to thrombin

Height data was gathered by taking 50 cross-section heights for each chemical species using two different images. A t-test was conducted without assuming equal variances to determine if the height data is significantly different. The p-value for the t-test was less than 0.0005 for the thrombin-aptamer pair. This indicates that the probability of accepting the null hypothesis (that the heights before and after binding are the same) was less than 0.05%. Therefore, the heights before and after binding are significantly different. The p-value for the control t-test and the poly A-poly T t-test was greater than 0.05, which indicates that the height changes in these systems were not significantly different. The averages, 95% confidence intervals, and t-test results can be seen in Table 2.

Table 2: Microcontact printing height summary

Heights in nm	Poly A	Hybridized DNA	Thrombin Aptamer	Bound Thrombin	Control poly A	Control bound thrombin
95% CI upper bound	1.800	1.677	2.023	2.723	1.800	1.813
Average	**1.684**	**1.588**	**1.855**	**2.451**	**1.684**	**1.711**
95% CI lower bound	1.569	1.499	1.687	2.178	1.569	1.610
P-Value	0.59		0.00047		0.73	

Discussion

It can be concluded from the findings that this microcontact printing sensor system is sufficiently accurate to determine the binding ability of aptamers. In a sensor system, a printed aptamer array would be exposed to the desired protein and a height change would indicate the presence of an aptamer on the array with sufficient specificity. A statistical

difference before and after binding must be shown in the height data before a printed array sensor system is feasible. In an array of aptamers, the high-affinity thrombin aptamer pair shows a sufficient height change to be detectable. The control pair of poly A-thrombin and poly A-poly T show a non-significant height change, which clearly indicates that the measured height changes for the complementary thrombin pair are due to binding events.

It is predictable that the binding of poly A and poly T does not result in a height change, as complementary DNA strands would not build structures vertically unless they are of different lengths. While the single-stranded poly A DNA would have little or no structure, the hybridized DNA would form a stiff helical rod. Unless the formation of the rod caused the DNA to "stand up" relative to the substrate, no major difference in height would be seen between the single- and double-stranded DNA.

The well-documented "coffee ring" effect is present in many of the images, and is due to the uneven drying of the DNA ink during the microcontact printing process. The ink has a tendency to concentrate on the stamp edges, which is seen in the figures. The ripple effect seen in some of the images is due to interference from the gold surface. It was necessary to use a narrow cantilever in order to achieve the desired sensitivity, which has a smaller deflection area than the size of the detection laser beam. As a result, the reflection of the laser beam from the sample surface creates a diffraction pattern on the detector (Lohmeyer, 2008).

The greatest hurdle to implementation of this system lies in the sample and AFM resolution. Previous work has shown heights of 1.7 ± 0.2 nm for single stranded DNA and 2.7 ± 0.3 nm for thrombin on freshly cleaved mica (Liu, Lin, Li, & Yan, 2005), and this work validates that previous experiment. Heights of 1.86 ± 0.2 nm for the thrombin aptamer and 2.45 ± 0.3 nm for the bound thrombin were found on the gold surface, although the sputter-coated gold is rougher than the mica surface used in the previous experiment (see table 3).

Table 3: Previous research height comparison

	Thrombin aptamer	Bound thrombin
Previous research	1.7 ± 0.2 nm	2.7 ± 0.3 nm
Current findings	1.86 ± 0.2 nm	2.45 ± 0.3 nm

The RMS roughness over a 10 μm square is 0.9 nm for the sputter-coated gold, while freshly cleaved mica has a roughness on the order of 0.13 nm (Senden & Ducker, 1992).

The concept of an AFM height-based sensor system has potential for a less specialized fluorescence-free alternative to current systems with applications to an inexpensive method of determining binding specificity with minimally modified aptamers and proteins. Based on the information obtained from the specificity test, the applicability of certain affinity pairs for small scale manufacturing methods could be determined.

By using the AFM rather than a fluorescence method to measure the printed aptamers, it was also shown that the microcontact printing method does not form highly dense monolayers. While fluorescence may show a fairly even luminescence in a printed area, the AFM measurements show a less uniform height distribution. This implies that the printed aptamers do not form self-assembled monolayers as easily or closely as with printed alkanethiols (Mrksich & Whitesides, 1995).

Future work will be to decrease noise in the system further, and to expand the sensor system to multi-aptamer arrays. Using thin film transfer or other methods for coating the gold may also result in a smoother surface to increase the contrast between the substrate and the printed material. The use of a polymer substrate for printing could also be investigated, in order to better encourage self-assembled monolayers to form. A printed layer of avidin, which is shown to form a closely packed self-assembled monolayer (Boujday et al., 2008), could be used as a substrate with a biotinylated thrombin aptamer. This study has shown that a sensor system with minimally modified DNA aptamers and unmodified protein is feasible using height changes and the atomic force microscope.

Chapter 3: The use of force spectroscopy to measure thrombin-aptamer interaction

A paper to be submitted to *Langmuir*

Janice Marquardt, Pranav Shrotriya, Marit Nilsen-Hamilton

Abstract

As the use of chemical species to form nanostructures becomes ever more common, the need to detect binding specificity and strength of these species also increases. The strength of binding for a complementary species pair can determine its suitability for certain structures or sensor systems. The purpose of this study is to use the force spectroscopy (force microscopy) method to measure the force and specificity of the interaction between the anti-coagulation protein thrombin and the single-stranded DNA thrombin aptamer. This study used a 30-nt adenine oligonucleotide (Poly A) and 2 kDa poly(ethylene) glycol (PEG) as controls, and the thrombin DNA aptamer and thrombin for the targeted detection pair. The thiolated poly A, PEG, and aptamer were printed onto gold, and then repeatedly brought into contact with a thrombin-coated atomic force microscope (AFM) tip. It was shown that the binding force of the thrombin-aptamer interaction was 17.8 pN, and there was little or no response from the controls. The results from this experiment show that the thrombin-aptamer pair has far-reaching applications for biosensors and building nanostructures.

Introduction

In the development of micro and nanoscale structures and sensors, the forces between molecules are a key factor for determining molecule suitability. Low binding forces between a selected complementary pair of molecules can result in an instable nanostructure, or a lack of sensor sensitivity. DNA aptamers are a chemical species that behave similarly to antibodies, and are selected from a random pool to bond to specific proteins (Cullen & Greene, 1989). These aptamers have high affinity for their complementary proteins, but frequently rely on lesser binding such as physical confirmation or Van der Waals forces to bind protein (Cullen & Greene, 1989; Ellington & Szostak, 1990). Shortly after the first

aptamers were developed, it became apparent that there was a need to measure the force of their interaction to determine suitability to specific applications.

Nearly fifteen years ago, a method to directly measure binding forces between specific complementary chemical species using the atomic force microscope (AFM) was discovered and put into practice (Florin, Moy, & Gaub, 1994). This method—coined force spectroscopy or force microscopy—has been used to determine the binding specificity and force for biotin-avidin (Florin, Moy, & Gaub, 1994), alkanethiols (Oncins, Vericat, & Sanz, 2008), single-stranded DNA pairs (Strunz, Oroszlan, Schäfer, & Güntherodt, 1999), and many other complementary chemical species. Binding forces for these interactions were determined to be in the range of 30 to 150 pN (Basnar, Elnathan, & Willner, 2006), which verified that many aptamer-protein pairs were suitable for nanostructures or biosensors.

Biosensors use a variety of methods to detect the prescence of a certain protein, including chemical assays, Love-wave sensors (Gronewold, Glass, Quandt, & Famulok, 2005), charge transfer sensors (Hianik, 2005), or microcantilever sensors (Lavrik, Sepaniak, & Datskos, 2004). While chemical assays and charge transfer sensors are not as dependent on binding forces for detection, wave sensors and microcantilever sensors require high specificity in binding and stable binding forces for detection. The proteins detected using this system are found in the bloodstream, and so are normally found in low concentration heterogeneous mixtures of many proteins and molecules. One such protein is the coagulation protein thrombin, which is instrumental in the synthesis of fibrin from fibrinogen during the blood clotting process.

Thrombin has a wide range of health effects in the human system, from thrombosis caused by too much fibrin in the system to hemorrhage sometimes caused by too little fibrin in the bloodstream. Thrombin also has a documented aptamer, which has been shown in chemical assays to have high binding specificity (Bode et al., 1989; Tasset, Kubik, & Steiner, 1997; Tsiang, Gibbs, Griffin, Dunn, & Leung, 1995). These two factors make the thrombin-aptamer pair both relevant for the study of binding forces and suitable for force spectroscopy.

In this paper, we study the forces between human thrombin and a 35-nt thrombin aptamer using the force spectroscopy method. This force was previously found by Basnar et

al. to be about 4.45 pN, and we follow a similar method with some small modifications to further demonstrate binding specificity (Basnar, Elnathan, & Willner, 2006).

Methods

Unless otherwise noted, all chemicals were purchased from Sigma Aldrich (www.sigma.com), and all DNA oligos were purchased from Integrated DNA Technologies (www.idtdna.com).

To functionalize the AFM tip, a carboxyl-coated (COOH) silicon nitride tip was purchased from Novascan Technologies, Inc. (www.novascan.com). Tip spring constants were calibrated by Novascan to minimize error in calculations. Each experiment used a fresh AFM tip, prepared using the following method: First, the probe was incubated in freshly prepared 10 mg/mL carbodiimide (EDAC) in double distilled water (ddH_2O) for 30 minutes. Then the probe was washed twice in phosphate-buffered sodium chloride (PBS, pH 7.3). Human thrombin was prepared as 1 mg/mL in PBS and the probe was incubated in the thrombin solution for 90 minutes. Last, the probe was washed 3 times for 5 minutes each in PBS and 3 times for 5 minutes each in ddH_2O. The probe was either used immediately or stored for less than 24 hours in ddH_2O before use.

To verify the presence of thrombin on the AFM tip, contact angle measurements were made at each point in the preparation process. 500 nL of water was placed on the AFM cantilever substrate, and the contact angle was measured by taking a picture of the water droplet from the side. After the tip was submerged in the thrombin solution and rinsed, a notably more hydrophilic surface indicated that the thrombin was bonded to the AFM tip and substrate.

To coat the substrate with the thiolated thrombin aptamer (5'-thiol-GCC TTA ACT GTA GTA CTG GTG AAA TTG CTG CCA TTG GTT GGT GTG GTT GG-3' (Tasset, Kubik, & Steiner, 1997), a 1 mg/mL concentration of the aptamer in binding buffer (20 mM Tris-HCl pH 7.4, 140 nM NaCl, 5 mM KCl, 1 mM $CaCl_2$, 5 mM $MgCl_2$, and 5% glycerol v/v in ddH_2O) was heated to 55°C and then vortexed for 30 seconds. The aptamer solution was deposited on a silicon wafer with a 25 nm thick layer of sputter-coated gold for 30 seconds

and then the excess liquid was poured off. The sample was rinsed with ddH_2O several times and grounded with copper tape before being scanned by the AFM.

To print the thiolated poly A single stranded DNA (5'-AAA AAA AAA AAA AAA AAA AAA AAA AAA AAA-thiol-3'), a 1 mg/mL concentration of poly A in binding buffer (20 mM Tris-HCl pH 7.4, 140 nM NaCl, 5 mM KCl, 1 mM $CaCl_2$, 5 mM $MgCl_2$, and 5% glycerol v/v in ddH_2O) was heated to 55°C and then vortexed for 30 seconds. The poly A solution was deposited on a silicon wafer with a 25 nm thick layer of sputter-coated gold for 30 seconds and then the excess liquid was poured off. The sample was rinsed with ddH_2O several times and grounded with copper tape before being scanned by the AFM.

To print the thiolated poly(ethylene) glycol (PEG, 2 kDa, purchased from Creative PEGworks www.creativepegworks.com), a 1 mg/mL concentration of PEG in ethanol was heated to 45°C and vortexed for 30 seconds (Jans et al., 2004). The PEG solution was deposited on a silicon wafer with a 25 nm thick layer of sputter-coated gold for 30 seconds and then the excess liquid was poured off. The sample was rinsed with ddH_2O several times and grounded with copper tape before being scanned by the AFM.

Force curves were performed using a Dimension 3100 atomic force microscope in binding buffer (20 mM Tris-HCl pH 7.4, 140 nM NaCl, 5 mM KCl, 1 mM $CaCl_2$, 5 mM $MgCl_2$, and 5% glycerol v/v in ddH_2O) at 174.4 nm/s (0.872 Hz over 200 nm). For each substrate material, 10 samples were taken at each of 6 different locations on the substrate, for a total of 60 samples per material. Only the last binding event for each force curve was used for analysis, as that data likely has the fewest binding events. The data was processed using the data table export function of the NanoScope offline software version 5.30 and Microsoft Excel 2003.

Results

The results confirm high binding specificity between thrombin and the thrombin aptamer. Using two different methods, the binding force was calculated to be 17.8 pN and 106.5 pN. Characteristic force curves for each of the interactions are shown in Figures 9, 10 and 11.

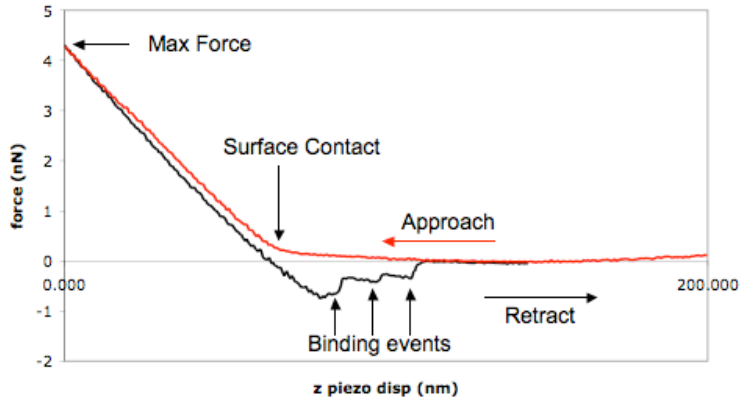

Figure 9: Characteristic thrombin aptamer force curve

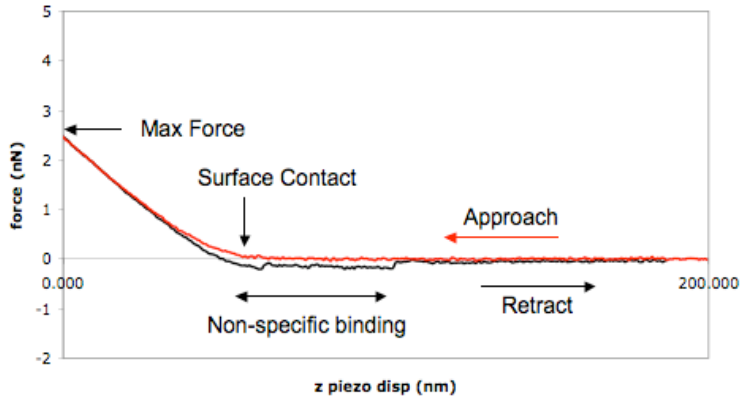

Figure 10: Characteristic non-specific binding (poly A) force curve

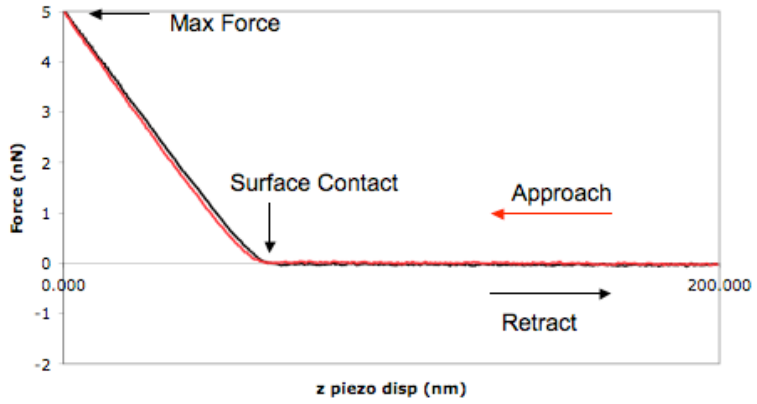

Figure 11: Characteristic non-binding (PEG) force curve

The first method uses a contact area calculation to correlate the gathered data to the expected number of bound molecules. A Hertz method was used to calculate the contact area using the equation:

$$A = \left(\frac{3FR}{4E^*}\right)^{\frac{1}{3}}$$ (Johnson, 1985)

where A is the contact area, R is the tip radius, F is the maximum force, and E* is the composite elastic modulus. The tip radius was found by scanning very sharp spikes with the AFM to characterize the tip shape. This scan was then programmed in MATLAB to determine the tip radius at the point of contact with the surface. Tip radii were found to be 10.7 nm for the aptamer tip, 13.9 nm for the poly A tip, and 7.9 nm for the PEG tip.

The composite elastic modulus was found by fitting the force displacement curve to the Hertzian contact model. The equation for the force displacement curve during contact is given by:

$$\delta = \left(\frac{9P^2}{16RE^{*2}}\right)^{1/3}$$ (Johnson, 1985)

where δ is the tip deflection and P is the contact force, and E* can be calculated from the graph of force versus deflection. An average of twenty data sets was taken to determine E* for the monolayer and gold combination. While many researchers use E* for solid gold, we found that the E* for the DNA monolayer on gold was significantly lower (~0.2 GPa) and so this calculation improves the accuracy and specificity of our calculations.

The density of thrombin was calculated based on a dense layer of ~3 nm diameter thrombin molecules, for a density of 1.1 x 10^{13} molecules per square centimeter. A theoretical 60% of the monolayer is assumed to account for surface artifacts, resulting in 6.6 x 10^{12} thrombin molecules per square centimeter. The surface coverage of the thiolated thrombin aptamer was determined with microgravimetric measurments to be 6 x 10^{12} molecules per square centimeter (Basnar, Elnathan, & Willner, 2006). Based on a chemical assay conducted using a thrombin aptamer of similar length in a similar binding buffer solution, a binding rate of 27% was used for all calculations (Mokhtarian, 2004).

The contact area calculated with the Hertz contact method was then expanded to include all interactions where the tip and substrate were within 4.4 nm of contact. This is because AFM height measurements showed that the aptamer monolayer has a thickness of 1.9 nm, and the protein monolayer has a thickness of 2.5 nm (see Chapter 2). A calculated average of 5.15 molecules were in contact for each binding event, for a calculated force of 106.5 pN per thrombin-aptamer bond. This number was derived from the previously described contact mechanics methods.

Histograms of the thrombin aptamer and poly A substrate experiments are shown in Figures 12 and 13, respectively. A bin size of four was used because it is sufficiently low to avoid sampling above the Nyquist frequency, and sufficiently high to show a trend. It can be seen from the histograms that the non-specific binding does not show a regular trend, so no further analysis was done on the non-specific binding data. The non-binding data did not even show meniscus or Van der Waals forces due to the repellant nature of PEG and protein, so there was insufficient data to generate a histogram.

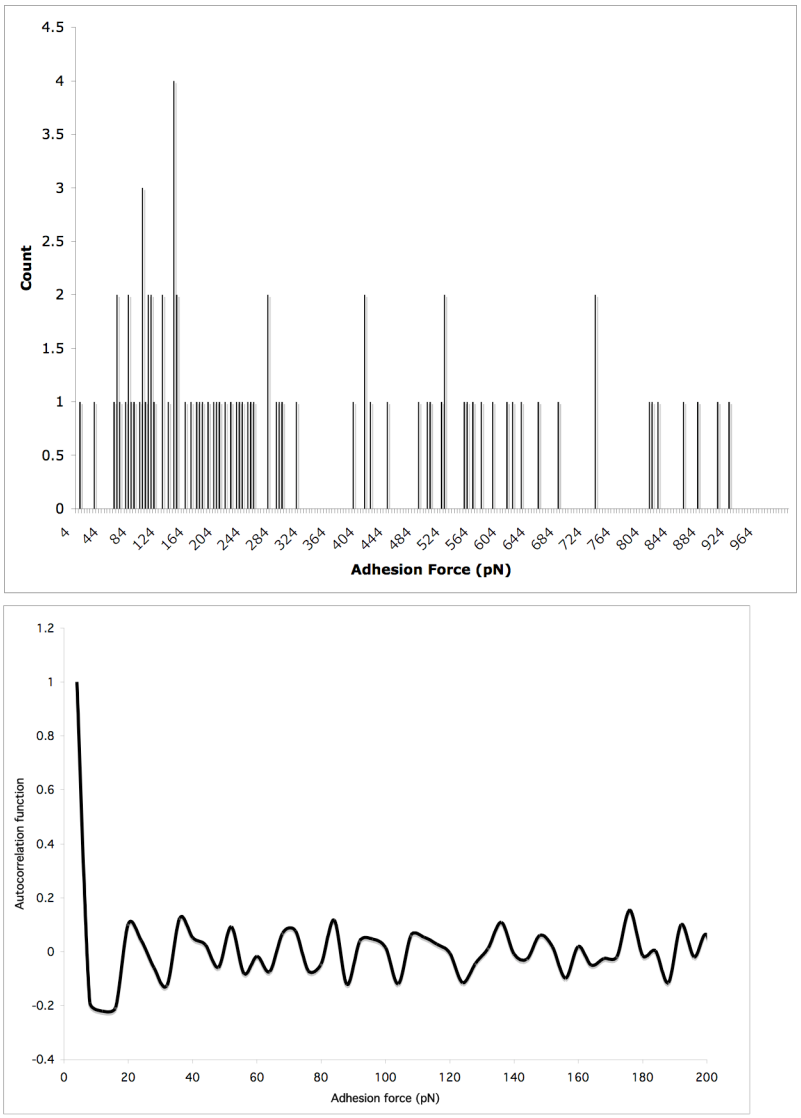

Figure 12: aptamer histogram and autocorrelation function

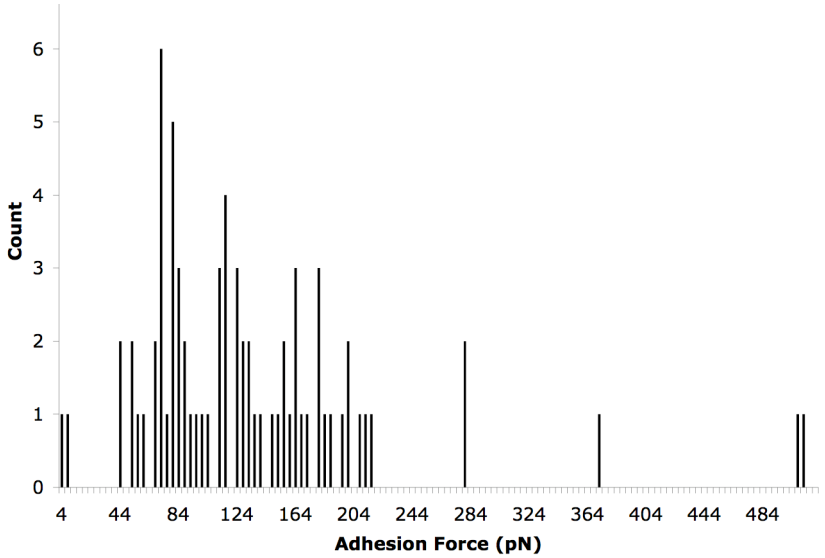

Figure 13: Poly A histogram

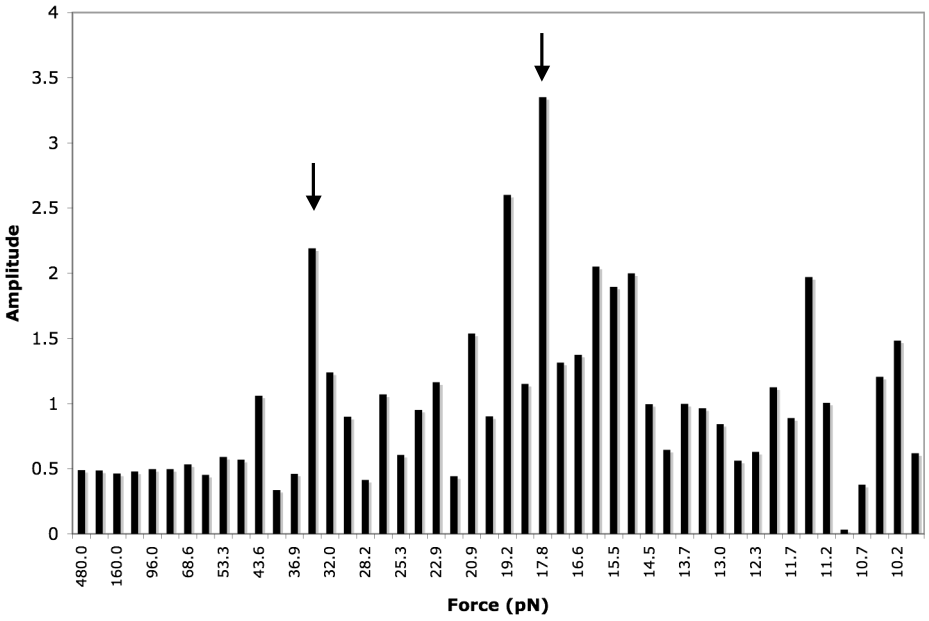

Figure 14: Force Spectroscopy Fourier Analysis. Arrows denote force quantum locations.

After subjecting the data to a smoothing function (Marchand & Marmet, 1983), an autocorrelation function was applied to the aptamer data (see Figure 12) to determine the force quantum of the data. Multiple frequencies appeared in the autocorrelation function, so a Fourier analysis was applied (see Figure 14) to find a force quantum of 17.8 pN. This quantum was similar across the data, regardless of bin size used in the analysis.

The peaks seen in the histogram were also graphed linearly with respect to the number of binding events (see Figure 15). The slope of this line is 17.7 pN per binding event with a coefficient of determination (R^2) of 0.997, which correlates well with the Fourier analysis.

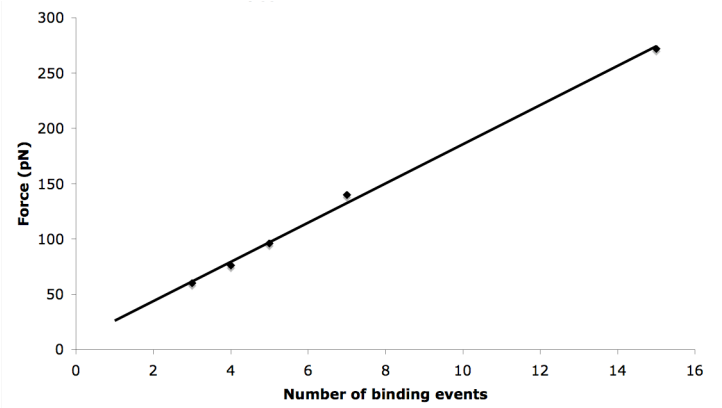

Figure 15: Linear regression of the specific binding adhesion force peaks

Discussion

This experiment showed a difference from the work of Basnar et al., who showed a bond strength of 4.5 pN for the same aptamer-protein complementary pair (Basnar, Elnathan, & Willner, 2006). While there may be many causes for this discrepancy, we hypothesize that it is due to differences in the assumptions made for each experiment.

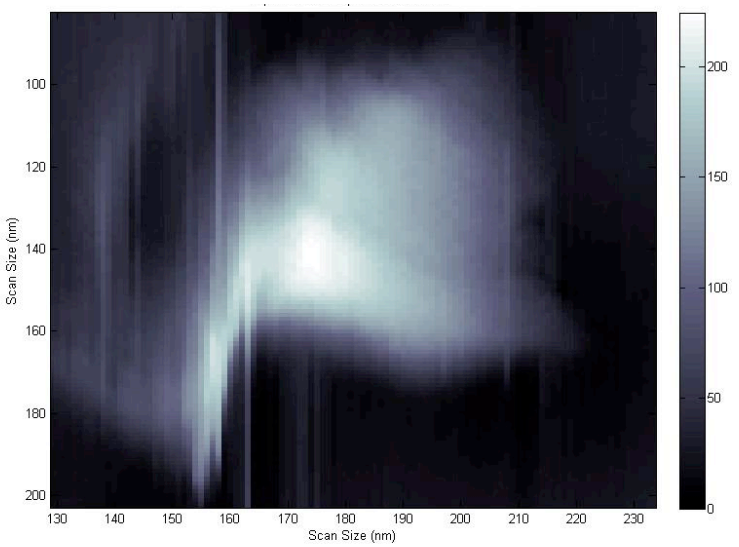

Figure 16: Aptamer AFM tip characterization

The nominal tip radius of 30 nm was found through tip characterization to be 10.7 nm for the aptamer data (see Figure 16). This resulted in far fewer bonds per interaction and so increased the calculated force. The calculated value for E* for the monolayers is much lower than that of gold, which showed that contact mechanics methods cannot be neglected. A

simple geometric interpretation of the contact does not account for the deformation of the monolayers. The histogram bin size can also have a large impact on force data analysis. The autocorrelation function and Fourier analysis reduce the error due to bin size, and the data was also calculated for a range of bin sizes to determine trends independent of bin size. The scale of the histogram of the previous experiment has a maximum measured force of 100 pN, while this experiment has a scale of nearly 1000 pN. Previous force spectroscopy experiments are on the scale of 1000 pN (Florin, Moy, & Gaub, 1994). Non-specific binding forces for this experiment were on the range of 200 pN. The prior research also determines a 60% binding rate, which is quite high for this interaction. Chemical assays show a binding rate of closer to 27.5% (Mokhtarian, 2004).

In reconciling the differences between the contact mechanics model and the Fourier analysis, there are several possibilities for the discrepancy in the calculated forces. The contact mechanics value of 106.5 pN per bond is based on a Hertzian contact model with the added radius from interactions less than 4.4 nm apart. This measurement was determined experimentally, but it is difficult to find the true separation of tip and substrate where bonding occurs. This calculation is also highly dependent on the concentration of aptamers on the surface, which was determined by others through microgravimetric measurements to be 6×10^{12} molecules per square centimeter (Basnar, Elnathan, & Willner, 2006). Small changes in the concentration yield large changes in the calculated adhesion force. It is also notable that 106.5 pN is very near the sixth force quantum of 17.8 pN (106.8 pN).

Future work for characterizing the thrombin-aptamer bond forces could investigate the effects of changing variables on the calculated forces. Research has shown that the pull-off speed in force spectroscopy experiments can affect the measured forces by as much as 10-fold (Taubenberger et al., 2007). Further investigation into the physical properties of the thrombin and thrombin aptamer monolayers would also yield greater accuracy in the calculations of adhesion forces using contact mechanics methods. This experiment reinforced the specificity of the thrombin-aptamer binding complex, and has increased the depth of analysis initially conducted by Basnar et al (Basnar, Elnathan, & Willner, 2006).

Chapter 4: General Conclusions

General Discussion

Through investigation of the interactions between the thrombin aptamer (Tasset, Kubik, & Steiner, 1997) and the blood coagulation protein thrombin, it has been shown that there is sufficiently high binding force and specificity between these chemical species for their use in nanoscale manufacturing and biosensors. The proof-of-concept sensor system using a microcontact printing array has shown that the atomic force microscope can be used with minimally modified aptamer-protein complexes to detect binding specificity.

Recommendations for Future Work

Future work for the microcontact sensor will be to decrease noise in the system further, and to expand the sensor system to multi-aptamer arrays. An array printed of several different aptamers would further demonstrate specificity and improve speed of identification. It could also detect secondary, less specific aptamers with lower binding forces.

Using thin film transfer or other methods for coating the gold may also result in a smoother surface to increase the contrast between the substrate and the printed material. The use of a polymer substrate for printing could also be investigated, in order to better encourage self-assembled monolayers to form. A printed layer of avidin or another chemical species could be used as a substrate with a biotinylated thrombin aptamer. While mica and glass are possibilities for fluorescent sensors, they could also be investigated as height change sensor substrates to increase the flexibility of the system.

Future work for the aptamer-thrombin forces should evaluate the effects of retraction speed on the measured force. Previous work has shown that different retract speeds during pull-off can change force measurements by as much as 10-fold (Taubenberger et al., 2007). Further investigation into the physical properties of the thrombin and thrombin aptamer monolayers such as their thicknesses and moduli of elasticity would also yield greater accuracy in the calculations of adhesion forces using contact mechanics methods.

Acknowledgements

I would first like to thank Dr. Pranav Shrotriya for his help as my advisor. I chose my advisor first and my project second, and have not regretted that decision. My committee members Dr. Sriram Sundararajan and Dr. Marit Nilsen-Hamilton have been very helpful in their advice on how to conduct experiments and their troubleshooting abilities. Without Dr. Nilsen-Hamilton's biochemistry expertise, I would not have any results. Thank you especially to Virginia and William Binger, whose endowed assistant professorship for Dr. Shrotriya provided funding for this project.

I would also like to thank Kyungho Kang, Kanaga Karuppiah (KK) and Ashish Sachan for tolerating me even as an undergraduate, and for aiding me in the physical execution of parts of my experiments. Bob Doyle, Warren Straszheim, and David Schmidt are all lab technicians for the many facilities I needed to complete this work, and their knowledge in their respective areas was most helpful.

Thank you to my mother Denise Hayward, my father John Gustafson, and my stepfather Michael Carter for encouraging me to pursue a graduate degree and for understanding when I reach my limits. Thank you to Daniela Faas for being a mentor to me and for her proofreading skills. Allison Machtemes and the other ladies on the 2007 cabinet of the Society of Women Engineers Iowa State section also deserve a shout out for their continual moral support and for making my daily life worthwhile. Last, but not least, thank you to my husband Ryan Marquardt for his support and for having to go through this process just a little before me to pave my way and always remind me why I am where I am today. He kept our life moving forward during this process and continually provides me with vision and a larger view of the world.

Appendix A: Poly(ethylene) Glycol Superstructure

In conducting the force spectroscopy experiment, a notable pattern was observed with the atomic force microscope (AFM) on the poly(ethylene) glycol (PEG) surface (See Figure 17). While superstructures of PEG which look similar to those seen in Figure 17 have been seen (Rathore & Sogah, 2001), this structure was much larger than previously documented.

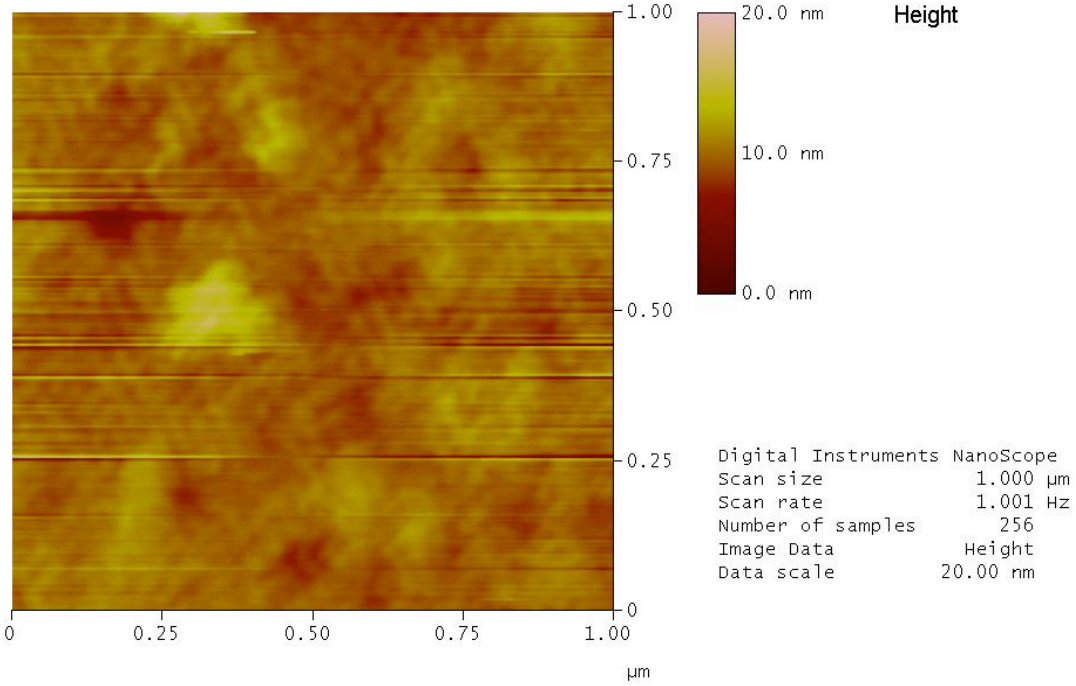

Figure 17: PEG superstructure surface

The diagonal pattern that formed would suggest at least one very dense monolayer, with other layers possibly building on the base monolayer. It is unlikely that this structure is the result of a scanning artifact, as other scans of other materials and shapes conducted that day with that same tip did not show the same patterns. Assuming the results seen in Figure 17 are repeatable, the superstructure seen here may be worthy of further investigation.

Appendix B: Force Spectroscopy Aptamer Data

The data shown is for the last pull-off event in each force curve. The bond force is calculated based on the proportion of the last event as part of the total pull-off event.

Point #	File #	Lower Point (nN)	Higher Point (nN)	Event Force (pN)	Proportion of total pull-off	Calculated bond force (pN)
2	38	-0.9845	-0.9090	75.5000	0.1823	83.2561
3	39	-0.8404	-0.5702	270.2000	1.0000	54.1391
4	40	-0.5873	-0.2973	290.0000	1.0000	57.9714
5	41	-0.6141	-0.4265	187.6000	1.0000	37.5529
7	42	-1.116	-0.9065	209.5000	0.4320	96.8000
9	43	-0.9138	-0.8432	70.6000	0.2100	67.0178
10	44	-0.7774	-0.4947	282.7000	1.0000	56.3357
11	45	-0.8871	-0.4825	404.6000	1.0000	80.7198
13	46	-0.7945	-0.6945	100.0000	0.3230	61.7028
15	47	-0.4606	-0.4069	53.7000	0.1385	77.4248
16	49	-1.123	-0.5166	606.4000	1.0000	118.1650
17	50	-1.106	-0.2534	852.6000	1.0000	167.7787
18	51	-1.309	-0.5020	807.0000	1.0000	158.6362
21	52	0.151	0.1754	24.4000	0.0254	189.8600
23	53	-0.129	0.1048	233.8000	0.3297	139.9347
24	54	-0.9797	-0.1048	874.9000	1.0000	172.8921
26	55	-0.307	-0.2485	58.5000	0.0636	181.5975
28	56	-0.4094	-0.3533	56.1000	0.0432	256.1429
31	57	-0.551	-0.4581	92.9000	0.1020	179.5706
32	58	-1.355	-0.5386	816.4000	1.0000	160.7011
33	59	-1.421	-0.5191	901.9000	1.0000	177.3252
35	60	-0.6629	-0.5824	80.5000	0.1365	118.0356
36	62	-0.5922	-0.4143	177.9000	1.0000	37.1746
40	63	-0.9456	-0.8724	73.2000	0.1267	121.5237
42	64	-0.9748	-0.8798	95.0000	0.2334	85.3748
43	65	-1.172	-0.3631	808.9000	1.0000	168.0945
45	66	-0.4362	-0.3265	109.7000	0.3062	74.8615
46	67	-0.4947	-0.3729	121.8000	1.0000	25.5189
47	68	-1.5743	-1.0550	519.3000	1.0000	97.1337
48	69	-1.8106	-1.2233	587.3000	1.0000	112.0751
50	70	-1.3818	-1.2258	156.0000	0.2667	111.3911
52	71	-1.238	-1.1746	63.4000	0.1066	113.0832
53	72	-1.685	-1.1380	547.0000	1.0000	104.3590
55	73	-1.679	-1.1868	492.2000	0.4988	187.8799
56	74	-1.3647	-0.8066	558.1000	1.0000	107.0348
57	75	-1.1161	-0.4655	650.6000	1.0000	124.7434
58	76	-1.551	-0.6312	919.8000	1.0000	175.4016
59	77	-0.9602	-0.3339	626.3000	1.0000	119.3035
60	78	-0.8042	-0.1901	614.1000	1.0000	116.7161
62	79	-0.909	-0.6385	270.5000	0.3172	161.1619
63	80	-0.7896	-0.3534	436.2000	1.0000	82.0777
64	81	-1.2209	-0.6507	570.2000	1.0000	107.3647
65	82	-1.2697	-0.7189	550.8000	1.0000	103.7787
67	85	-0.8042	-0.6994	104.8000	0.1920	103.6711
69	86	-0.8919	-0.7189	173.0000	0.3737	88.0263
72	87	-0.8944	-0.7579	136.5000	0.1965	132.5081
75	88	-1.172	-1.0480	124.0000	0.1621	146.0389
76	89	-1.233	-0.9821	250.9000	1.0000	47.4466
77	90	-1.121	-0.8749	246.1000	1.0000	47.0683
79	91	-0.9358	-0.7335	202.3000	0.4511	86.0661
82	93	-1.439	-1.3355	103.5000	0.2597	77.5675
83	94	-1.043	-0.6287	414.3000	1.0000	79.5100
84	95	-1.043	-0.6361	406.9000	1.0000	77.9128
85	96	-1.2599	-0.7457	514.2000	1.0000	98.5082
88	97	-1.0966	-0.9284	168.2000	0.2937	110.1152
90	98	-1.3379	-1.1990	138.9000	0.3064	87.1500
91	99	-1.1698	-0.7798	390.0000	1.0000	74.7271
92	100	-0.8698	-0.6774	192.4000	1.0000	36.9025
95	101	-1.489	-1.3525	136.5000	0.2467	105.3699
97	102	-0.9187	-0.7798	138.9000	0.3117	85.2519
100	103	-1.1113	-0.9139	197.4000	0.2219	171.1152
102	104	-0.9529	-0.7335	219.4000	0.3273	128.2633
103	105	-1.431	-0.7019	729.1000	1.0000	138.8858
105	106	-0.9894	-0.6799	309.5000	0.4847	122.0163
106	107	-0.9772	-0.4800	497.2000	1.0000	95.4117
108	108	-1.314	-1.2234	90.6000	0.4415	39.2198
109	109	-1.3257	-0.8066	519.1000	1.0000	99.3886
110	110	-1.5329	-1.0503	482.6000	1.0000	91.8419
113	111	-0.8919	-0.7847	107.2000	0.1448	140.7354
115	112	-0.9577	-0.8140	143.7400	0.1661	164.3998
117	113	-0.9139	-0.8213	92.6000	0.2695	65.3101
119	114	-0.9943	-0.8505	143.8000	0.2151	126.8418
120	115	-1.1039	-0.8724	231.5000	1.0000	44.1630
122	116	-1.235	-0.9943	240.7100	0.3445	133.2679
123	117	-1.6937	-0.9626	731.1000	1.0000	139.5279
124	118	-2.437	-1.7595	677.5000	1.0000	129.4692
125	119	-1.3842	-1.0966	287.6000	1.0000	55.2276
128	122	-0.9212	-0.8432	78.0000	0.1270	117.2277
129	123	-0.9626	-0.8335	129.1000	1.0000	24.7594
132	124	-1.106	-0.9456	160.4000	0.2485	123.9856
134	125	-0.9261	-0.8261	100.0000	0.2869	66.9693
136	126	-1.216059	-1.2101	5.9590	0.0185	61.9473
137	128	-0.9967	-0.7725	224.2000	1.0000	43.2116

Appendix C: References

Basnar, B., Elnathan, R., & Willner, I. (2006). Following aptamer-thrombin binding by force measurements. *Analytical Chemistry, 78*(11), 3638-3642.

Bock, L., Griffin, L., Latham, J., Vermaas, E., & Toole, J. (1992). Selection of single-stranded DNA molecules that bind and inhibit human thrombin. *Nature, 355*, 564-566.

Bode, W., Mayr, I., Baumann, U., Huber, R., Stone, S., & Hofsteenge, J. (1989). The refined 1.9 Å crystal structure of human a-thrombin: Interaction with D-Phe-Pro-Arg chloromethylketone and significance of the Tyr-Pro-Pro-Trp insertion segment. *The EMBO Journal, 8*(11), 3467-3475.

Boujday, S., Bantegnie, A., Briand, E., Marnet, P.-G., Salmain, M., & Pradier, C.-M. (2008). In-depth investigation of protein adsorption on gold surfaces: Correlating the structure and density o the efficiency of the sensing layer. *Journal of Physical Chemistry B, 112*, 6708-6715.

Chandross, M., Lorenz, C., Stevens, M., & Grest, G. (2008). Simulations of nanotribology with realistic probe tip models. *Langmuir, 24*, 1240-1246.

Cullen, B., & Greene, W. (1989). Regulatory pathways governing HIV-1 replication. *Cell, 58*, 423-426.

Dimitriadis, E., Horkay, F., Maresca, J., Kachar, B., & Chadwick, R. S. (2002). Determination of elastic moduli of thin layers of soft material using the atomic force microscope. *Biophysical Journal, 82*, 2798-2810.

Ellington, A. D., & Szostak, J. W. (1990). In vitro selection of RNA molecules that bind specific ligands. *Nature, 346*(6287), 818-822.

Feng, C. L., Embrechts, A., Vancso, G. J., & Schönherr, H. (2006). Reactive μCP on ultrathin block copolymer films: Localized chemistry for micro- and nano-scale biomolecular patterning. *European Polymer Journal, 42*, 1954-1965.

Feng, X.-z., Hou, S., Chan, Q.-l., Wang, L.-k., Qin, M., & Han, P.-d. (2004). Microcontact printing techniques in bioscience. *Chemical Research in Chinese Universities, 20*(6), 826-832.

Florin, E.-L., Moy, V., & Gaub, H. (1994). Adhesion forces between individual ligand-receptor pairs. *Science, 264*(5157), 415-417.

Goss, C., Brumfield, J., Irene, E., & Murray, R. (1993). Imaging and modification of Au(111) monatomic steps with atomic force microscopy. *Langmuir, 9*, 2986-2994.

Gronewold, T. M. A., Glass, S., Quandt, E., & Famulok, M. (2005). Monitoring complex formation in the blood-coagulation cascade using aptamer-coated SAW sensors. *Biosensors and Bioelectronics, 20*, 2044-2052.

Hianik, T. (2005). Detection of aptamer-protein interactios using QCM and electrochemical indicator methods. *Bioorganic & Medicinal Chemistry Letters, 15*, 291-295.

Jans, K., Bonroy, K., De Palma, R., Reekmans, G., Jans, H., Laureyn, W., et al. (2004). Stability of mixed PEO-Thiol SAMs for biosensing applications. *Langmuir, 24*, 3949-3954.

Johnson, K. L. (1985). *Contact Mechanics*. Cambridge: Cambridge University Press.

Kelly, J., Feigon, J., & Yeates, T. (1996). Reconciliation of the X-ray and NMR structures of the thrombin-binding aptamer d(GGTTGGTGTGGTTGG). *Journal of Molecular Biology, 256*, 417-422.

Kopycinska-Müller, M., Geiss, R., & Hurley, D. (2005). Contact mechanics and tip shape in AFM-based nanomechanical measurements. *Ultramicroscopy, 106*, 466-474.

Kumar, A., & Whitesides, G. (1993). Features of gold having micrometer to centimeter dimensions can be formed through a combination of stamping with an elastomeric stamp and an alkanethiol "ink" followed by chemical etching. *Applied Physics Letters, 63*(14), 2002-2004.

Lavrik, N., Sepaniak, M., & Datskos, P. (2004). Cantilever transducers as a platform for chemical and biological sensors. *Review of Scientific Instruments, 75*(7), 2229-2253.

Lee, J.-O., So, H.-M., Jeon, E.-K., Chang, H., Won, K., & Kim, Y. H. (2007). Aptamers as molecular recognition elements for electrical nanobiosensors. *Analytical and Bioanalytical Chemistry, 390*(4), 1023-1032.

Liu, Y., Lin, C., Li, H., & Yan, H. (2005). Aptamer-directed self-assembly of protein arrays on a DNA nanostructure. *Angewandte Chemie International Edition, 44*, 4333-4338.

Lohmeyer, L. (2008). Optical interference, alignment, subtraction. In J. Marquardt (Ed.) (pp. Personal Email). Ames, IA.

Macaya, R., Schultze, P., Smith, F., Roe, J., & Feigon, J. (1993). Thrombin-binding DNA aptamer forms a unimolecular quadraplex structure in solution. *Proceedings of the National Academy of Sciences of the United States of America, 90*, 3745-3749.

Marchand, P., & Marmet, L. (1983). Binomial smoothing filter: A way to avoid some pitfalls of least-squares polynomial smoothing. *Review of Scientific Instruments, 54*(8), 1034-1041.

Micic, M., Chen, A., Leblanc, R. M., & Moy, V. (1999). Scanning electron microscopy studies of protein-functionalized atomic force microscopy cantilever tips. *Scanning, 21*(6), 394-397.

Mokhtarian, M. (2004). *Gene expression detection using targeted reversibly activated prove (TRAP).* Iowa State University, Ames, IA.

Mrksich, M., & Whitesides, G. (1995). Patterning self-assembled monolayers using microcontact printing: A new technology for biosensors? *Tibtech, 13*, 228-235.

Noy, A., Vezenov, D., & Lieber, C. (1997). Chemical force microscopy. *Annual Review of Materials Science, 27*, 381-421.

Olsen, B. J., & Markwell, J. (2007). Assays for the determination of protein concentration. *Current Protocols in Protein Science*, 14-17.

Oncins, G., Vericat, C., & Sanz, F. (2008). Mechanical properties of alkanethiol monolayers studied by force spectroscopy. *The Journal of Chemical Physics, 128*, 044701.

Rathore, O., & Sogah, D. (2001). Nanostructure formation through β-sheet self-assembly in silk-based materials. *Macromolecules, 34*, 1477-1486.

Reedy, E. D., Jr. (2006). Thin-coating contact mechanics with adhesion. *Journal of Materials Research, 21*(10), 2660-2668.

Ruiz, S. A., & Chen, C. (2007). Microcontact printing: A tool to pattern. *Soft Matter, 3*, 168-177.

Senden, T., & Ducker, W. (1992). Surface roughness of plasma-treated mica. *Langmuir, 8*, 733-735.

Strunz, T., Oroszlan, K., Schäfer, R., & Güntherodt, H.-J. (1999). Dynamic force spectroscopy of single DNA molecules. *Proceedings of the National Academy of Sciences of the United States of America, 96*, 11277-11282.

Tasset, D., Kubik, M., & Steiner, W. (1997). Oligonucleotide inhibitors of human thrombin that bind distinct epitopes. *Journal of Molecular Biology, 272*, 688-698.

Taubenberger, A., Cisneros, D., Friederichs, J., Puech, P.-H., Muller, D., & Franz, C. (2007). Revealing early steps of $\alpha_2\beta_1$ integrin-mediated adhesion to collagen type I by using single-cell force spectroscopy. *Molecular Biology of the Cell, 18*, 1634-1644.

Thibault, C., Séverac, C., Mingotaud, A.-F., Vieu, C., & Mauzac, M. (2007). Poly(dimethylsiloxane) contamination in microcontact printing and its influence on patterning oligonucleotides. *Langmuir, 23*, 10706-10714.

Tsiang, M., Gibbs, C. S., Griffin, L., Dunn, K. E., & Leung, L. L. K. (1995). Selection of a suppressor mutation that restores affinity of an oligonucleotide inhibitor for thrombin using in vitro genetics. *Journal of Biological Chemistry, 270*(33), 19370-19376.

Tuerk, C., & Gold, L. (1990). Systematic evolution of ligands by exponential enrichment: RNA ligands to bacteriophage T4 DNA polymerase. *Science, 249*(4968), 505-510.

Watson, J. D., & Crick, F. H. C. (1953). Molecular Structure of Nucleic Acids. *Nature, 171*(4356), 737-738.

Xia, Y., & Whitesides, G. (1998). Soft lithography. *Annual Review of Material Science, 28*, 153-184.

Yang, M., Yau, H., & Chan, H. L. (1998). Adsorption kinetics and ligand-binding properties of thiol-modified double-stranded DNA on a gold surface. *Langmuir, 14*, 6121-6129.

Zhou, D., Bruckbauer, A., Ying, L., Abel, C., & Klenerman, D. (2003). Building three-dimensional surface biological assemblies on the nanometer scale. *Nano Letters, 3*(11), 1517-1520.